Material and Methods

Clinical samples

Ninety-three CRC patients underwent surgical treatment at the Kyushu University at Beppu and affiliated hospitals between 1993 and 1999. Resected tumor and paired nontumor tissue specimens were immediately cut from resected colon and placed in RNAlater (Takara, Japan) or embedded in Tissue Tek OCT medium (Sakura, Tokyo, Japan), or frozen in liquid nitrogen and kept at −80°C until RNA extraction. Written informed consent was obtained from all patients. The median follow-up period was 3.0 years.

Quantitative RT-PCR

The sequences of *FBXW7* mRNA primers were as follows: sense, 5′-AAA GAG TTG TTA GCG GTT CTC G-3′; antisense, 5′-CCA CAT GGA TAC CAT CAA ACT G-3′. Glyceraldehyde-3-phosphate dehydrogenase (*GAPDH*) was used as an internal control and *GAPDH* primers were as follows: sense, 5′-TTG GTA TCG TGG AAG GAC TCT A-3′; antisense, 5′-TGT CAT ATT TGG CAG GTT-3′. Real-time monitoring of PCR reactions was performed using the LightCycler™ system (Roche Applied Science, Indianapolis, IN) and SYBER-Green I dye (Roche Applied Science, Indianapolis, IN). Monitoring was performed according to the manufacturer's instructions, as described previously.[8] In brief, a master mixture was prepared on ice, containing 1 μL of cDNA, 2 μL of DNA Master SYBER-Green I mix, 50 ng of primers and 2.4 μL of 25 mM $MgCl_2$. The final volume was adjusted to 20 μL with water. After the reaction mixture was loaded into glass capillary tubes, quantitative RT-PCR was performed with the following cycling conditions: initial denaturation at 95°C for 10 min, followed by 40 cycles of 95°C for 10 sec, annealing at 62°C for 10 sec and extension at 72°C for 10 sec. After amplification, products were subjected to a temperature gradient from 67°C to 95°C at 0.2°C/sec, under continuous fluorescence monitoring, to produce a melting curve of products.

Data analysis for Quantitative RT-PCR

We used the LightCycler® Software version 3.5 program (Roche Molecular Biochemicals) to calculate the cycle numbers. After proportional baseline adjustment, the fit point method was employed to determine the cycle in which the log-linear signal was first distinguishable from the baseline. This cycle number was used as the crossing point value. A standard curve was produced by measuring the crossing point of each standard value and plotting it against the logarithmic concentration value. Concentrations of unknown samples were calculated by plotting their crossing points against the standard curve and dividing by *GAPDH* content. *GAPDH* expression levels were the same in tumor and normal tissues.

Immunohistochemistry

Immunohistochemical studies for FBXW7, c-Myc and cyclin E were performed on formalin-fixed, paraffin-embedded surgical sections obtained from 71 patients with CRC. Tissue sections were deparaffinized, soaked in 0.01 M sodium citrate buffer and boiled in a microwave for 5 min at 500 W to retrieve cell antigens. The primary mouse monoclonal antibodies against FBXW7 (Abnova Corporation, Taipei, Taiwan), mouse monoclonal antibodies against c-Myc (sc-40, Santa Cruz Biotechnology, CA) and rabbit polyclonal antibodies against Cyclin E (SC-481, Santa Cruz Biotechnology) were used at dilutions of 1:100, 1:50 and 1:50, respectively. Tissue sections were immunohistochemically stained using ENVISION reagents (ENVISION+ Dual Link System-HRP, Dako Cytomation, Glostrup, Denmark). All sections were counterstained with hematoxylin. We confirmed the specificity of antibody for *FBXW7* using by the thymus of *Fbxw7* knockout mouse established by Onoyama *et al.*[7] (Supporting Information, Fig. 4).

Laser microdissection

The tissues from another series of 130 patients with CRC were collected for laser micro-dissection (LMD). CRC tissues were microdissected using the LMD system (Leica Laser Microdissection System, Leica Microsystems, Wetzlar, Germany) as previously described.[9] For LMD, 5 μ frozen sections were fixed in 70% ethanol for 30 sec, stained with hematoxylin and eosin and dehydrated as follows: 5 sec each in 70%, 95% and 100% ethanol and a final 5 min in xylene. Sections were air-dried, then microdissected with the LMD system. Target cells were excised, at least 100 cells per section, and bound to the transfer film, and total DNA extracted.

cDNA-microarray

We used the commercially available Human Whole Genome Oligo DNA Microarray Kit (Agilent Technologies, Santa Clara, CA). A list of genes on this cDNA microarray is available from http://www.chem.agilent.com/scripts/generic.asp?lpage=5175 &indcol=Y&prodcol=Y&prodcol=N&indcol=Y&prodcol=N. Cyanine (Cy)-labeled cRNA was prepared using T7 linear amplification as described in the Agilent Low RNA Input Fluorescent Linear Amplification Kit Manual (Agilent Technologies). Labeled cRNA was fragmented and hybridized to an oligonucleotide microarray (Whole Human Genome 4 × 44K Agilent G4112F). Fluorescence intensities were determined with an Agilent DNA Microarray Scanner and were analyzed using G2567AA Feature Extraction Software Version A.7.5.1 (Agilent Technologies), which used the LOWESS (locally weighted linear regression curve fit) normalization method.[10] This microarray study followed MIAME guidelines issued by the Microarray Gene Expression Data group.[11] Further analyses were performed using GeneSpring version 7.3 (Silicon Genetics, San Carlos, CA).

Array-CGH

Array-CGH was performed using the Agilent Human Genome Microarray Kit 244K (Agilent Technologies). The array-CGH platform is a high resolution 60-mer oligonucleotides based

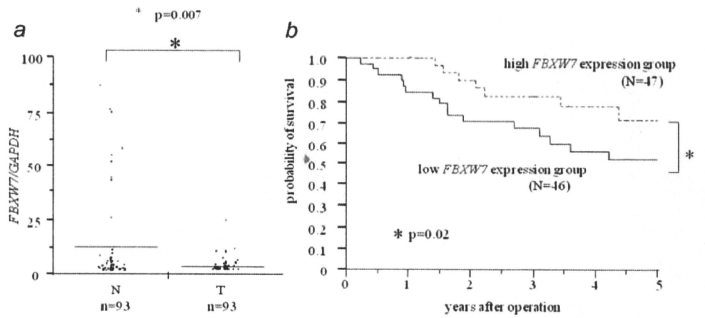

Figure 1. Clinical significance of *FBXW7* mRNA expression in CRC. (*a*) *FBXW7* mRNA expression in cancerous and normal tissues from CRC patients as assessed by real-time quantitative PCR ($n = 93$). Horizontal lines indicate mean value of each group (T, cancer tissue; N, noncancerous tissue). (*b*) Kaplan-Meier five year overall survival curves for CRC patients according to the level of *FBXW7* mRNA expression. The overall survival rate for patients in the high expression group was significantly higher than that for patients in the low expression group ($p = 0.02$). High expression group (broken line: $N = 47$), low expression group (unbroken line: $N = 46$).

microarray containing about 244,400 probes spanning coding and non-coding genomic sequences with median spacing of 7.4 kb and 16.5 kb, respectively. Labeling and hybridization were performed according to the protocol provided by Agilent (Protocol v4.0, June 2006). Arrays were analyzed using The Agilent DNA microarray scanner.

Array-CGH data analysis

The raw signal intensities of tumor DNAs were measured with Human Genome CGH Microarray 244K (Agilent Technologies) which were then transformed into log ratio to reference DNA with 'Feature Extraction' software (v9.1) of Agilent Technologies. The log ratio was thereafter used as the signal intensity of each probe. One hundred thirty samples from different patients were subjected to circular binary segmentation (CBS) after median normalization.[12] An R script written by us was used for the median normalization, whereas an R program implemented in the "DNA copy" package of the Bioconductor project (http://www.bioconductor.org) was used for the CBS analysis. Instead of all of the CGH probes, 13,403 probes from chromosome 4 (NCBI Build 35) were analyzed in this study. An absolute log2 ratio >0.263 was used as the threshold for the gain or loss in DNA copy number for each probe.

Total RNA extraction and first-strand cDNA synthesis

Frozen tissue specimens or cultured cell lines at subconfluency were homogenized, and total RNA was extracted using the modified acid-guanidine-phenol-chloroform method as described previously.[13,14] Total RNA (8.0 μg) was reverse transcribed to cDNA using M-MLV RT (Invitrogen Corp. Carlsbad, CA).

Cell lines

The human CRC cell lines, LoVo and Colo 201, were obtained from the Japanese Collection of Research Bioresoureces (JCRB, Osaka, Japan). The cell lines were maintained in Ham's F-12 medium and RPMI1640 (Invitrogen Corp.) supplemented with 10% fetal bovine serum (Equitech-Bio, Kerrville, TX), 100 units/mL penicillin G and streptomycin (Invitrogen Corp.). The cells were incubated in 5% CO_2 at 37°C and passaged every three days.

FBXW7 RNA interference

FBXW7-specific siRNA (Silencer™ Predesigned siRNA) was purchased from Ambion, USA. siRNA oligomer was diluted with Opti-MEMI® Medium without serum (Invitrogen Corp.). The diluted siRNA oligomer was mixed with the diluted Lipofectamine™ RNAiMAX (Invitrogen Corp.) and incubated for 15 min at room temperature to allow siRNA-Lipofectamine™RNAiMAX complexes to form. Diluted logarithmic growth-phase LoVo cells without antibiotics were seeded at 2×10^5 cells/well in a final volume of 2 mL or 100 μL in 6 or 96 well flat bottom microtiter plates, respectively. The cells were incubated in a humidified atmosphere (37°C and 5% CO_2). The assay was performed after 72 hr incubation.

Table 1. *FBXW7* mRNA expression and clinocopathological factors

	High expression (n = 47)		Low expression (n = 46)		
Factors	n	%	n	%	p value
Age (mean ± SD)	67.4 ± 10.0		67.4 ± 11.6		0.98
Sex					0.07
Male	30	63.8	22	47.8	
Female	17	36.2	24	52.2	
Histological grade					0.42
Well	19	40.4	14	30.4	
Moderately, poorly others	28	59.6	32	69.6	
Size					0.32
>30 mm (small)	10	21.3	11	23.9	
<31 mm (large)	37	78.7	35	76.1	
Depth of tumor invasion[1]					0.03
m, sm, sp	36	78.3	27	57.5	
s, se, si	10	22.7	20	42.5	
Lymph node metastasis					0.76
Absent	21	44.7	20	43.5	
Present	26	55.3	26	56.5	
Lymphtic invasion					0.59
Absent	29	61.7	25	54.3	
Present	18	38.3	21	45.7	
Venous invasion					0.23
Absent	43	91.5	38	82.6	
Present	4	8.5	8	17.4	
Liver metastasis					0.48
Absent	44	93.6	41	89.1	
Present	3	6.4	5	10.9	
Peritoneal dissemination					0.24
Absent	47	100.0	45	97.8	
Present	0	0.0	1	2.2	
Duke's stage					0.47
A, B	23	50.0	27	57.5	
C, D	3	50.0	20	42.5	

[1]Tumor invasion of mucosa (m), submucosa (sm), muscularis propria (mp), subserosa (ss), penetration of serosa (se), and invasion.

Western blot analysis

Total protein was extracted from cell lines using protein extraction solution (PRO-PREP, iNtRON Biotechnology, Korea). Total protein (40 μg) was electrophoresed in 10% concentrated READY GELS J (Bio-Rad Laboratories, Japan) and electroblotted onto pure nitrocellulose membranes (Trans-Blot Transfer Medium; Bio-Rad Laboratories, Japan) at 0.2 A for 120 min. c-Myc protein was detected using mouse monoclonal antibodies (sc-40, Santa Cruz Biotechnology) diluted 1:500. Cyclin E protein was detected using rabbit polyclonal antibodies (SC-481, Santa Cruz Biotechnology) diluted 1:100. c-Myc and cyclin E protein levels were normalized to the level of β-actin protein (Cytoskeleton, Denver CO) diluted 1:1,000. Blots were developed with horse-radish peroxidase-linked anti-mouse and rabbit immunoglobulin (Promega, Madison, WI) diluted 1:1,000. ECL Detection Reagents (Amersham Biosciences, Piscataway, NJ) were used to detect antigen-antibody reactions.

Proliferation assay

Proliferation of the cell lines was determined by 3-(4, 5-dimethylthiazol-2-yl)-2, 5-diphenyl tetrazolium bromide (MTT)

Table 2. Univariate and multivariate analysis for overall survival (Cox proportional regression model)

	Univariate analysis			Multivariate analysis		
Factors	**RR**	**95% CI**	***p* value**	**RR**	**95% CI**	***p* value**
Age (<65/<66)	0.820	0.540–1.218	0.328	–	–	–
Sex (male/female)	0.822	0.538–1.228	0.342	–	–	–
Histology grade (well/moderately and poorly & others)	0.690	0.416–1.063	0.095	–	–	–
Tumor size (<30 mm/>31 mm)	1.285	0.792–2.380	0.331	–	–	–
Depth of tumor invasion[1] (m, sm, mp/ss, se, si)	1.738	1.101–3.024	0.016	1.78	1.075–3.095	0.023
Lymph node metastasis(negative/positive)	2.014	1.329–3.231	0.001	2.145	1.368–3.563	0.001
Lymphatic invasion (negative/positive)	2.326	1.529–3.744	0.001	–	–	–
Venous invasion (negative/positive)	1.852	1.145–2.845	0.014	1.825	1.106–2.891	0.020
FBXW7 mRNA expression (low/high)	1.564	1.027–2.516	0.036	1.983	1.264–3.267	0.003

[1]Tumor invasion of mucosa (m), submucosa (sm), muscularis propria (mp), subserosa (ss), penetration of serosa (se), and invasion of adjacent strucures (si). Abbreviations: RR, relative risk; CI, confidence interval.

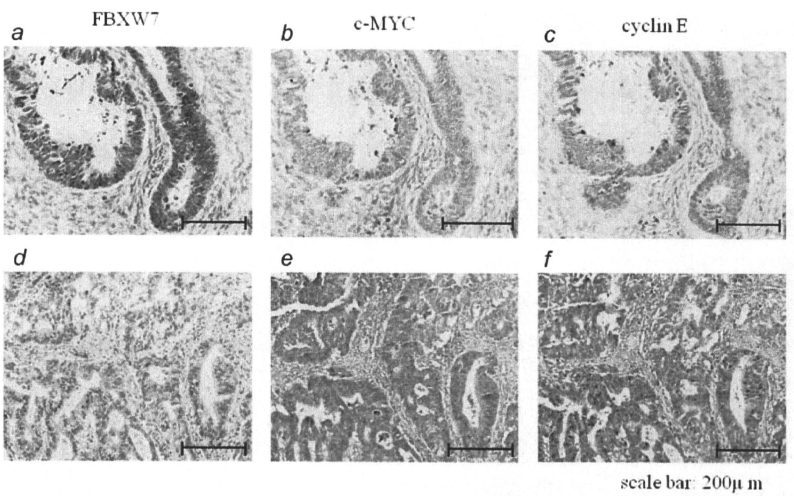

Figure 2. Immunohistochemical analysis of FBXW7, c-MYC and cyclin E expression in CRC. In cases of high FBXW7 protein expression (*a*), there was no detectable c-MYC (*b*) or cyclin E (*c*) protein expression in the same tissue section. In contrast, in the case of low FBXW7 protein expression (*d*), there was strong c-MYC (*e*) and cyclin E (*f*) protein expression (×200 original magnification). [Color figure can be viewed in the online issue, which is available at www.interscience.wiley.com.]

assay (Roche Diagnostics GmbH, Mannheim, Germany). After 24 hr incubation with siRNA, cells were seeded at 5×10^3 cells well^{-1} in microtiter plates (96 wells, flat bottom) in a final volume of 100 μL culture medium per well, in a humidified atmosphere (37°C and 5% CO_2). After 72 hr incubation, 10 μL of MTT labeling agent (final concentration 0.5 mg mL^{-1}) was added to each well. The microtiter plate was incubated for 4 hr in a humidified atmosphere. Solubilization solution (100 μL) was added to each well. The plate was allowed to stand overnight in the incubator in a

humidified atmosphere. After checking for complete solubilization of the purple formazan crystals, spectrophotometric absorbance of the sample was measured using a model 550 microplate reader (Bio-Rad Laboratories, CA), at a wavelength of 570 nm corrected 655 nm. Each independent experiment was performed three times.

Statistical analysis

For continuous variables, data were expressed as the mean ± standard deviation. The relationship between *FBXW7* mRNA expression and clinicopathological factors was analyzed using a χ^2 test and Student's *t*-test. Overall survival curves were plotted according to the Kaplan-Meier method and the generalized Log-rank test was applied to compare the survival curves. All tests were analyzed using JMP software (SAS Institute Inc., Cary, NC) and the findings were considered significant for p values <0.05.

Results

Expression of FBXW7 mRNA in clinical tissue specimens

FBXW7 mRNA expression was examined in 93 CRC clinical samples using reverse transcription-polymerase chain reaction (RT-PCR) and real-time quantitative RT-PCR, with quantified values used to calculate *FBXW7/GAPDH* ratios. In these samples, clinicopathological factors, including prognosis, were available. The mean expression level of *FBXW7* mRNA in tumor tissue specimens was significantly lower than that of nontumor tissue ($p = 0.007$) (Fig. 1*a*).

FBXW7 mRNA expression and clinicopathological characteristics

We divided the 93 CRC cases into two groups according to the median tumor (*T*)/normal (*N*) ratio of *FBXW7* mRNA expression level as determined above. Thus, 46 cases were placed in the high *FBXW7* expression group and 47 cases in the low *FBXW7* expression group. The association between clinicopathological features and *FBXW7* mRNA expression is summarized in Table 1. In the low *FBXW7* expression group, tumor invasion was significantly elevated compared to the high *FBXW7* expression group ($p = 0.02$). Univariate analysis identified *FBXW7* expression, tumor invasion, lymph node metastasis, lymphatic invasion and venous invasion as prognostic factors for 5-year overall survival following surgery. Variables with p values <0.05 by univariate analysis were selected for multivariate analysis using Cox's proportional hazards model. *FBXW7* expression [relative risk (RR): 1.98, confidence interval (CI): 1.26–3.26, $p = 0.003$] was found to be a significant factor affecting five year overall survival following surgery (Table 2). Analysis of 5-year overall survival curves showed that patients in the low *FBXW7* expression group had a significantly poorer prognosis than those in the high expression group ($p = 0.02$) (Fig. 1*b*).

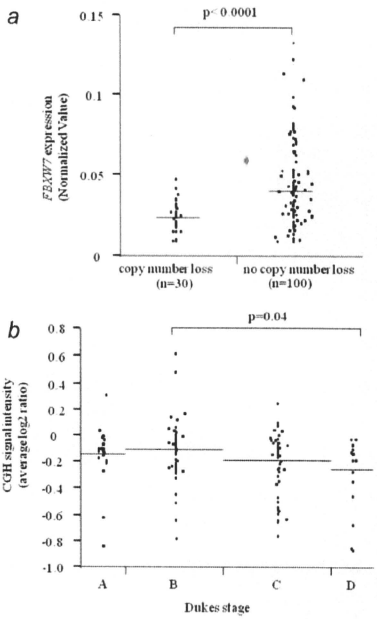

Figure 3. Concordant loss of *FBXW7* expression and copy number alteration in the flanking region of *FBXW7*. There were 30 cases with deletions and 100 cases without loss in CRC. The expression of *FBXW7* in the deleted cases was significantly lower than the cases with wild type *FBXW7* ($p < 0.0001$). (*a*) CGH signal intensity (average log2 ratio) according to Dukes staging classification. (*b*) The ratio of copy number loss of *FBXW7* increased along with the progression of Dukes' stage.

Immunohistochemical determination of FBXW7, c-MYC and cyclin E expression

Expression of FBXW7 protein was evaluated by immunohistochemistry of resected CRC specimens, using an anti-FBXW7 antibody. When FBXW7 protein was expressed at high levels, expression of c-MYC and cyclin E protein was below detection (Figs. 2*a–c*). This patient had a 5-year, recurrence-free survival after curative surgery despite the advanced stage. In contrast, in cases of low FBXW7 protein expression, strong expression of c-MYC and cyclin E proteins was noted (Figs. 2*d–f*). This patient died from peritoneal dissemination six months after curative surgery. We examined the association between *FBXW7* and *c-MYC* or *Cyclin E* in serial

Table 3. The copy number loss of *FBXW7* and clinocopathological factors

Factors	Copy number loss group (n = 30)		No abberant group (n = 100)		p value
	n	%	n	%	
Age (mean ± SD)	67.4 ± 10.0		67.4 ± 10.0		0.293
Sex					0.107
Male	13	43.3	60	60.0	
Female	17	56.7	40	40.0	
Histological grade					0.439
Well	15	50.0	58	58.0	
Moderately, poorly others	15	50.0	42	42.0	
Size					0.157
>30 mm (small)	8	26.7	15	15.0	
<31 mm (large)	22	76.3	85	85.0	
Depth of tumor invasion[1]					1.000
m, sm, sp	24	80.0	80	80.0	
s, se, si	6	20.0	20	20.0	
Lymph node metastasis					0.049
Absent	11	36.7	57	57.0	
Present	19	63.3	43	43.0	
Lymphtic invasion					0.021
Absent	8	26.7	50	50.0	
Present	22	73.3	50	50.0	
Venous invasion					0.049
Absent	7	2.3.3	42	42.0	
Present	23	76.7	58	58.0	
Liver metastasis					0.098
Absent	24	80.0	91	91.0	
Present	6	20.0	9	9.0	
Peritoneal dissemination					0.683
Absent	29	96.7	98	98.0	
Present	1	3.3	2	2.0	
Duke's stage					0.045
A, B	10	33.3	54	54.0	
C, D	20	66.7	46	46.0	

[1]Tumor invasion of mucosa (m), submucosa (sm), muscularis propria (mp), subserosa (ss), penetration of serosa (se), and invasion of adjacent strucures (si).

sections of 71 cases by immunohistochemical study. Seventy one CRC samples were divided into three groups according to *FBXW7* protein level (high = 16, medium = 19 and low = 36). We compared the expression between *FBXW7* protein and mRNA in 52 cases with high and low *FBXW7* protein level. The expression level of *FBXW7* mRNA in high *FBXW7* protein group (n = 16) is significantly higher than that in low *FBXW7* protein group (n=36) (Supporting Information 3*a*, p = 0.03). Furthermore, we found the significant inverse correlation between *FBXW7* and *c-MYC* or *cyclin E*. (supporting information, Fig. 3*b*: *FBXW vs. c-MYC*: $r = -0.526$, $p < 0.0001$, *FBXW7 vs. cyclin E*: $r = -0.553$, $p < 0.0001$).

Aberrations in FBXW7 copy number in CRC specimens

To clarify the cause of suppression of *FBXW7* mRNA in patients with poorer prognosis, we investigated copy number aberrations of *FBXW7* in 130 CRC specimens using laser micro-dissection and CGH array. As shown in Figure 3*a*, there was a significant correlation between expression of *FBXW7* and copy number of the *FBXW7* region (Fig. 3*a*) ($p < 0.0001$). Therefore, loss of *FBXW7* expression described

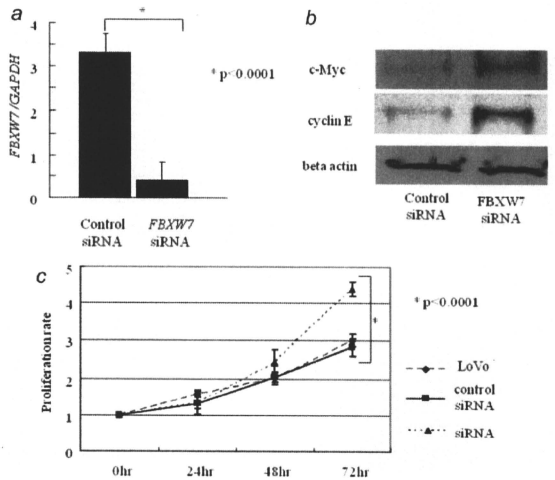

Figure 4. Effect of *FBXW7* gene silencing on a colon cancer cell line. (*a*) *FBXW7* mRNA in LoVo cells was suppressed by *FBXW7* siRNA as confirmed by quantitative RT-PCR. (*b*) Expression of c-MYC and cyclin E proteins was enhanced by *FBXW7* siRNA, as confirmed by Western blot analysis. These proteins were normalized to the level of beta actin. (*c*) The proliferation rate of LoVo cells treated with *FBXW7* siRNA (dotted line) was significantly greater than that in control siRNA cells (unbroken line) and parent LoVo cells (broken line).

above was caused by genetic alteration in the flanking region of *FBXW7*. Figure 3*b* shows CGH signal intensity (average log2 ratio) according to Dukes staging classification (Supporting Information, Fig. 1: heat map representation of copy number aberration of *FBXW7* according to Dukes staging classification). Thirty cases (23.1%) had at least one copy number aberration in all cases. The ratio of copy number loss of *FBXW7* increased along with the progression of Dukes' stage. The association between clinicopathological features and the copy number of *FBXW7* is summarized in Table 3. In the copy number loss group, lymphatic invasion, venous invasion and lymph node metastasis was increased compared with the nonaberrant group (Table 3, $p = 0.02$, $p = 0.04$ and $p = 0.04$, respectively). In addition, the copy number loss group had more advanced cases compared with the nonaberrant group ($p = 0.04$).

Effect of FBXW7 gene silencing on CRC cell lines

LoVo cells expressed *FBXW7* mRNA at a high level as confirmed by RT-PCR. We examined whether suppression of *FBXW7* would enhanced c-Myc and cyclin E protein expression, both of which are degradation targets of *FBXW7*. The expression level of *FBXW7* mRNA was suppressed by *FBXW7*-specific siRNA as confirmed by RT-PCR analysis (Fig. 4*a*). We found that the protein expression levels of c-Myc and cyclin E were enhanced by *FBXW7*-specific siRNA as confirmed by Western blotting analysis (Fig. 4*b*). Furthermore, we evaluated the proliferation activity of LoVo cells suppressed by *FBXW7*-specific siRNA using MTT assays. We found that the proliferation rate in LoVo cells suppressed by *FBXW7* siRNA significantly increased compared to that in control cells (Fig. 4*c*). We demonstrated that similar phenomena are found in Colo 201 (Supporting Information, Fig. 5).

Discussion

In our current study, we found that *FBXW7* mRNA gene expression was significantly suppressed in human CRC tissue compared to the corresponding normal tissue ($p = 0.007$) and that the patients in the low *FBXW7* expression group had a significantly poorer prognosis than those in the high expression group ($p = 0.02$). We also examined how loss of *FBXW7* contributed to cell growth.

We found that approximately 25% of patients with CRC have a reduced copy number of *FBXW7*, and that the incidence of genetic alteration was concordantly increased with the progression of disease stage. Tsafrif *et al.* and Lassmann *et al.* previously reported that particular chromosomal

regions and genes that are frequently gained and overexpressed (e.g., 7p, 8q, 13q and 20q) or lost and underexpressed (e.g., 1p, 4, 5q, 8p, 14q, 15q and 18).[15,16] Our current array-CGH data is consistent with their previous data (Supporting Information, Fig. 2). Chromosome 4q, containing the *FBXW7* gene, is deleted in various carcinomas such as esophageal, gastric, and breast cancer.[17,18] Rajagopalan *et al.* previously reported that the deficiency of *FBXW7* in CRC is associated with genetic instability.[19] The mutations in *FBXW7* in colorectal tumor have been found in 6–8%.[19,20] However, Kemp *et al.* suggested that mutations in *FBXW7* in colorectal tumor do not affect the chromosomal instability and result in biallelic inactivation.[20] We found that *FBXW7* was altered at the genetic level in CRC as determined by LMD and CGH array. Our findings that *FBXW7* gene copy number loss frequently occurred in CRC may provide insight into how *FBXW7* function is inactivated during cancer development.

The decrease of FBXW7 expression gave rise to abnormal accumulation of c-MYC and cyclin E protein.[21] MYC protein plays crucial roles in mitogenic and cell growth responses and is commonly deregulated in cancers.[22] Cyclin E is a key component of the cell cycle machinery that is frequently deregulated in cancer.[23] Our current study indicated that FBXW7 regulates c-MYC and cyclin E *in vitro*. In fact, it appears that FBXW7 normally inhibits c-Myc and cyclin E and thereby promotes exit from the cell cycle at G1-S phase. Those findings suggest that *FBXW7* may be a tumor suppressor gene and loss of the gene could prevent cells from entering a quiescent state. Thus, it is possible that introduction of *FBWX7* gene or protein could force tumors into dormancy.

According to Figure 3*a*, all CRC cases with genetic alterations exhibited diminished *FBXW7* expression. However, 65 cases (65%) in Figure 3*a* showed loss of *FBXW7* expression without genetic alteration. To explain this finding, we speculate theremay be epigenetic transcriptional regulation,[24] translational regulation by non-coding RNA or upregulation of Wnt/beta-catenin signals from interstitial niche cells associated with cancer cells.

In conclusion, multivariate analysis showed that *FBXW7* expression in CRC is an independent prognostic factor for five year survival following surgery. *FBXW7* may be useful as a prognostic indicator in CRC. Cell cycle regulation by ubiquitin ligase has potential in developing new targets in cancer therapy.

Acknowledgements

We thank Ms. T. Shimooka, Mrs. K. Ogata, Ms. M. Kasagi, Ms. Y. Nakagawa and Ms. T. Kawano for their technical assistance. The novelty and impact of this article is that we firstly investigated the copy number aberrations of FBXW7 in a series of 130 human colorectal cancer (CRC) specimens with laser microdissection by comprehensive genome hybridization (CGH) array and FBXW7 gene expression in another subset of 93 CRC samples with clinicopathlogic factors, including prognosis. Furthermore, those identified findings of the clinicopathologic significance of FBXW7 repression was validated biologically by CRC cell line with siRNA interference, which showed FBXW7 repression accelerated the cell cycle to determine a prognostic factor in CRC cases.

References

1. Bashir T, Pagano M. Aberrant ubiquitin-mediated proteolysis of cell cycle regulatory proteins and oncogenesis. *Adv Cancer Res* 2003;88:101–44.
2. Akhoondi S, Sun D, von der Lehr N, Apostolidou S, Klotz K, Maljukova A, Cepeda D, Fiegl H, Dafou D, Marth C, Mueller-Holzner E, Corcoran M, et al. FBXW7/hCDC4 is a general tumor suppressor in human cancer. *Cancer Res* 2007;67:9006–12.
3. Mao JH, Perez-Losada J, Wu D, Delrosario R, Tsunematsu R, Nakayama KI, Brown K, Bryson S, Balmain A. Fbxw7/Cdc4 is a p53-dependent, haploinsufficient tumour suppressor gene. *Nature* 2004;432:775–9.
4. Welcker M, Clurman BE. FBW7 ubiquitin ligase: a tumour suppressor at the crossroads of cell division, growth and differentiation. *Nat Rev Cancer* 2008;8:83–93.
5. Sonoda H, Inoue H, Ogawa K, Utsunomiya T, Masuda TA, Mori M. Significance of skp2 expression in primary breast cancer. *Clin Cancer Res* 2006;12:1215–20.
6. Nakayama KI, Nakayama K. Ubiquitin ligases: cell-cycle control and cancer. *Nat Rev Cancer* 2006;6:369–81.
7. Onoyama I, Tsunematsu R, Matsumoto A, Kimura T, de Alboran IM, Nakayama K, Nakayama KI. Conditional inactivation of Fbxw7 impairs cell-cycle exit during T cell differentiation and results in lymphomatogenesis. *J Exp Med* 2007;204:2875–88.
8. Ogawa K, Utsunomiya T, Mimori K, Tanaka F, Inoue H, Nagahara H, Murayama S, Mori M. Clinical significance of human kallikrein gene 6 messenger RNA expression in colorectal cancer. *Clin Cancer Res* 2005;11:2889–93.
9. Nishida K, Mine S, Utsunomiya T, Inoue H, Okamoto M, Udagawa H, Hanai T, Mori M. Global analysis of altered gene expressions during the process of esophageal squamous cell carcinogenesis in the rat: a study combined with a laser microdissection and a cDNA microarray. *Cancer Res* 2005;65:401–9.
10. Quackenbush J. Microarray data normalization and transformation. *Nat Genet* 2002;32 (Suppl):496–501.
11. Brazma A, Hingamp P, Quackenbush J, Sherlock G, Spellman P, Stoeckert C, Aach J, Ansorge W, Ball CA, Causton HC, Gaasterland T, Glenisson P, et al. Minimum information about a microarray experiment (MIAME)-toward standards for microarray data. *Nat Genet* 2001;29:365–71.
12. Venkatraman ES, Olshen AB. A faster circular binary segmentation algorithm for the analysis of array CGH data. *Bioinformatics* 2007;23:657–63.
13. Utsunomiya T, Hara Y, Kataoka A, Morita M, Arakawa H, Mori M, Nishimura S. Cystatin-like metastasis-associated protein mRNA expression in human colorectal cancer is associated with both liver metastasis and patient survival. *Clin Cancer Res* 2002;8:2591–4.
14. Utsunomiya T, Okamoto M, Hashimoto M, Yoshinaga K, Shiraishi T, Tanaka F, Mimori K, Inoue H, Watanabe G, Barnard GF, Mori M. A gene-expression signature can quantify the degree of hepatic fibrosis in the rat. *J Hepatol* 2004;41:399–406.
15. Lassmann S, Weis R, Makowiec F, Roth J, Danciu M, Hopt U, Werner M. Array CGH identifies distinct DNA copy number profiles of oncogenes and tumor

suppressor genes in chromosomal- and microsatellite-unstable sporadic colorectal carcinomas. *J Mol Med* 2007;85:293–304.
16. Tsafrir D, Bacolod M, Selvanayagam Z, Tsafrir I, Shia J, Zeng Z, Liu H, Krier C, Stengel RF, Barany F, Gerald WL, Paty PB, et al. Relationship of gene expression and chromosomal abnormalities in colorectal cancer. *Cancer Res* 2006;66:2129–37.
17. Sterian A, Kan T, Berki AT, Mori Y, Olaru A, Schulmann K, Sato F, Wang S, Paun B, Cai K, Hamilton JP, Abraham JM, et al. Mutational and LOH analyses of the chromosome 4q region in esophageal adenocarcinoma. *Oncology* 2006;70:168–72.
18. Takada H, Imoto I, Tsuda H, Sonoda I, Ichikura T, Mochizuki H, Okanoue T, Inazawa J. Screening of DNA copy-number aberrations in gastric cancer cell lines by array-based comparative genomic hybridization. *Cancer Sci* 2005;96:100–10.
19. Rajagopalan H, Jallepalli PV, Rago C, Velculescu VE, Kinzler KW, Vogelstein B, Lengauer C. Inactivation of hCDC4 can cause chromosomal instability. *Nature* 2004;428:77–81.
20. Kemp Z, Rowan A, Chambers W, Wortham N, Halford S, Sieber O, Mortensen N, von Herbay A, Gunther T, Ilyas M, Tomlinson I. CDC4 mutations occur in a subset of colorectal cancers but are not predicted to cause loss of function and are not associated with chromosomal instability. *Cancer Res* 2005;65:11361–6.
21. Welcker M, Singer J, Loeb KR, Grim J, Bloecher A, Gurien-West M, Clurman BE, Roberts JM. Multisite phosphorylation by Cdk2 and GSK3 controls cyclin E degradation. *Mol Cell* 2003;12:381–92.
22. Grandori C, Cowley SM, James LP, Eisenman RN. The Myc/Max/Mad network and the transcriptional control of cell behavior. *Annu Rev Cell Dev Biol* 2000;16:653–99.
23. Hwang HC, Clurman BE. Cyclin E in normal and neoplastic cell cycles. *Oncogene* 2005;24:2776–86.
24. Gu Z, Mitsui H, Inomata K, Honda M, Endo C, Sakurada A, Sato M, Okada Y, Kondo T, Horii A. The methylation status of FBXW7 beta-form correlates with histological subtype in human thymoma. *Biochem Biophys Res Commun* 2008;377:685–8.

Notch pathway as candidate therapeutic target in Her2/Neu/ErbB2 receptor-negative breast tumors

HAJIME HIROSE[1], HIDESHI ISHII[1,2], KOSHI MIMORI[2], DAISUKE OHTA[2], MASAHISA OHKUMA[1], HIROHIKO TSUJII[3], TOSHIYUKI SAITO[3], MITSUGU SEKIMOTO[1], YUICHIRO DOKI[1] and MASAKI MORI[1,2]

[1]Department of Gastrointestinal Surgery, Osaka University School of Medicine, Osaka; [2]Department of Molecular and Surgical Oncology, Medical Institute of Bioregulation, Kyushu University, Ohita; [3]Research Center for Charged Particle Therapy, National Institute for Radiological Science, Chiba, Japan

Received July 27, 2009; Accepted September 2, 2009

DOI: 10.3892/or_00000603

Abstract. Whereas the Her2/neu/erbB2 receptor (Her2) could be a molecular target of the receptor-positive breast cancer, the therapeutic targets of Her2-negative cancer largely remain to be established. The expression of Her2 was evaluated in 48 primary breast cancer tumors by immunohistochemistry. The identified Notch pathway was studied in genotoxin-dependent suppression of breast cancer-initiating cell growth. Immunohistochemical assessment of Her2-negative tumors revealed significant association with overexpression of Notch1 and Notch3. Knockdown of Notch pathway resulted in sensitization of breast cancer cells to deionizing radiation, leading to cell death; the effect was more significant in stem marker $CD44^+$ than in $CD44^-$ cells, and more profound in the Her2-negative than in positive cancer cells. The present study indicates that inhibition of Notch signaling could antagonize survival signal of Her2-negative breast cancer-initiating cells carrying genomic damage, and suggests that targeted suppression of the Notch pathway may give the rationale for sensitizing Her2-negative cancer-initiating cells to a therapeutic approach.

Introduction

Breast cancer is the most common type of carcinoma in women in the western world (1). Most patients with breast cancer have surgery to remove the cancer from the breast through breast-conserving surgery, an operation to remove the cancer but not the whole breast, including lumpectomy to remove a tumor lump with a small amount of surrounding normal tissue, and partial or segmental mastectomy to remove the part of the breast that contains cancer as well as some normal tissues. Lymph nodes are taken out to examine metastasis. Survival rates for breast cancer have been improving for >20 years: the estimated relative five-year survival rate for women diagnosed in western world in 2001-2003 was 80%, compared with only 52% for women diagnosed in 1971-1975 (2). The estimated relative 20-year survival rate for women with breast cancer has been improved from 44% in the early 1990s to 64% for the most recent period (2). After the relatively common local and rare (~2%) regional recurrences, as well as distant metastasis (involving bone in 25% of the cases), most physicians however have performed second-line treatments such as chemo- and hormone therapy (2). The efficacy of hormone therapy would be expected in hormone sensitive tumors, whereas the efficacy of chemotherapy is not easily predicted and may vary and depend on the case.

After gaining FDA (USA) approval in September 1998, trastuzumab, a humanized monoclonal antibody that acts on the Her2/neu/erbB2 (Her2), an epidermal growth factor (Egf)-like receptor, opened an avenue to the treatment of breast cancer patients whose tumors overexpress the gene product (3). Amplification of Her2 occurs in 25-30% of early-stage breast cancers (4). Although the Her2 signaling pathways induced by the receptor are incompletely characterized, it is reported that activation of the phosphoinositide 3-kinase/Akt pathway is involved and associated with mitogenic signaling involving the mitogen-activated protein kinase pathway, leading to promoting invasion, survival of tumor cells and angiogenesis (5). In the clinical trials leading up to the FDA approval, 42% of patients taking trastuzumab in combination with the chemotherapy drug paclitaxel had significant responses, although the succeeding studies indicated that the response rate for $Her2^+$ patients was only 30% and resistance developed rapidly, in virtually all patients, presumably through the mechanism of the lack of p27Kip1 translocation to the nucleus, enabling Cdk2 to induce cell proliferation (6). It is suggested that trastuzumab has a major impact in the treatment of Her2-positive metastatic breast cancer (7). In Her2-negative, recurrent cases, in which mechanisms other than receptor signaling might play a role in tumor development, the

Correspondence to: Dr Masaki Mori, Department of Gastroenterological Surgery, Osaka University, Graduate School of Medicine, Suita, Yamadaoka 2-2, Osaka 565-0871, Japan
E-mail: mmori@gesurg.med.osaka-u.ac.jp

Key words: Notch, ErbB2 receptor, breast tumors

biological efficacy of trastuzumab would not be expected, but novel molecular targets for Her2-negative cases and efficient therapeutic strategy would be desirable.

In the present study, we screened 48 primary breast cancer tumors for characterizing Her2-negative tumors by immunohistochemistry, which allowed the detection of the functional significance of Notch family proteins; an inverse correlation of Her2 with Notch proteins. Notch proteins are members of the conserved transmembrane receptor family, which play a role in cell fate decisions such as stem cell proliferation, differentiation and cell death (8). The Notch genes encode transmembrane receptors, which contain a large extracellular domain, composed of a variable number of Egf-like repeats and an intracellular signaling domain, which consists of six ankyrin/cdc10 motifs and nuclear localization signals (9). Notch receptors interact through their extracellular domain with other membrane-associated ligands, the Delta and Serrate/Jagged families, which are composed of five proteins, Jagged1 and 2 and Delta-like 1, 3 and 4 (9). Notch signaling is activated by ligand-receptor interaction and triggers proteolytic cleavages by the γ-secretase complex, which releases the Notch intracellular domain into the nucleus.

Notch intracellular domain binds to the Cbf1 DNA binding protein of the transcriptional activator complex, the activation of which can lead to the expression of target genes, such as Hes family genes, involved in cell growth and differentiation. In the present study, we show that the signal of Jagged-Notch-Cbf1 axis was involved in the survival of Her2-negative breast cancer initiating cells after exposure to genotoxic insults. Recent studies indicate significant involvement of the Notch signaling pathway in initiation and development of breast cancer (10-12). Whereas the oncogenic function of Notch1 and Notch14 is shown by studies of the mammary epithelial cell system (10-12), the animal experiment demonstrated that transgenic overexpression of the Notch intracellular domain of Notch1 and Notch3 resulted in the development of mammary tumors (13). Although a protein homology search indicated that Notch3 lacks the putative transactivation domain of Notch1, herein we focused on the study of the Notch1 and 3, and found that knockdown of Notch3, and to a lesser extent, Notch1 proteins resulted in sensitization to genotoxic, deionizing radiation. The effect was more apparent in $CD44^+$ breast cancer-initiating cells than in $CD44^-$ cells and more profound in Her2-negative than in positive cancer cells. Taken together, a possible role of Notch family is proposed as survival factors of Her2-negative breast cancer initiating cells, i.e., the protective role of cancer-initiating cells from the induction of cell death, which could lead to survival and accumulation of damaged cells carrying deleterious mutations.

Materials and methods

Primary tumors. Primary breast tumors from 48 female patients (average age 56 years old; range, 27-78) were obtained surgically in the Institute of Bioregulation Hospital, Kyushu University Hospital with written informed consent and under the control and approval of the institutional committees of research ethics. From all the cases, documented informed consents were obtained to use these excised specimens in the present research. The cohort includes 12 cases with scirrhous carcinoma, 20 cases with papillary tubular ductal carcinoma, 2 cases with solid tubular carcinoma, 2 cases with predominant intraductal component, a case of micropapillary pattern, a case of solid papillary type, a case of DCIS, 2 cases with spindle type, an unclassified case, 3 cases with invasive lobular carcinoma, 2 cases with mucinous invasive carcinoma, and a case of medullary carcinoma. Seventeen of 48 cases were premenopausal.

Cell culture. Her2-negative/dim human breast cancer MCF7 and Her2-positive HCC1419 cells were purchased from American Type Culture Collection (Manassas, VA) and cultured in RPMI medium supplemented with 10% FCS (14,15). Cells ($5x10^4$) in plastic dishes were cultured for 6 h with 25 μM L-685, 458 (Sigma-Aldrich, St. Louis, MO) as γ-secretase inhibitor, diluted in pre-warmed medium from a 10 mM stock prepared in dissolved in dimethylsulfoxide, and harvested to perform the protein study. For transfection, oligo siRNAs for Notch1, Notch3, CBF1, Jagged1, Jagged2, and luciferase as mock control were synthesized (Ambion-Applied Biosystems, Tokyo, Japan) and used for transfection as recommended, using TransIT-TKO transfection reagent (Mirus, Madison, WI). FACS was performed after $1x10^5$ cells were fixed with 70% ethanol for 10 min, incubated with RNase A, and stained with propidium iodide. The following monoclonal antibodies were used for flow cytometric study: mAbs against biotin-labeled CD44 (BD Bioscience, San Jose, CA). The CD44 positive and negative cells were probed with streptoavidin-coated magnetic beads and separated by the automated magnetic cell sorting (MACS; Miltenyi Biotec, Tokyo, Japan). For cell cycle analysis, the analysis was performed using a FACS multi-color detection system after ethanol-fixation and propidium iodide staining. For radiation, 60-70% confluent culture in dishes 10 cm in diameter were washed with PBS and irradiated at 4 Gy. Control cells were taken into the radiation exposure instrument similarly to irradiated cells, but not irradiated.

MTS proliferation assay. The CellTiter 96 AQueous assay, composed of solutions of tetrazolium compound [3-(4,5-dimethylthiazol-2-yl)-5-(3-carboxymethoxyphenyl)-2-(4-sulfophen yl)-2H-tetrazolium, inner salt; MTS] and an electron coupling reagent (phenazine methosulfate; PMS) (Promega, San Luis Obispo, CA), was used for detection of bio-reduction in a formazan product that is soluble in tissue culture medium. The absorbance of the formazan product at 490 nm was measured directly from 96-well assay plates, which correlate with cell number. Cells ($2x10^3$/well) were seeded and grown in 96-well plat bottom plates. The experiment was performed in triplicate and statistical evaluation was performed with Microsoft Excel (Microsoft Corp., Redmond, WA). Counts of viable cells by excluding trypan blue were well compatible with the MTS assay.

Real-time RT-PCR assays. Cells were dissected in cold phosphate-buffered saline, and total cellular RNAs were isolated with an RNeasy kit (Qiagen, Tokyo, Japan). Total RNA (1 μg) was used for TaqMan reverse-transcription (Applied Biosystems, Foster City, CA). Real-time PCR was performed in triplicate on an ABI Prism 7700 sequence

Table I. Immunohistochemical detections of Her2, Notch1 and Notch3.

	Notch1		Notch3	
Staining	Weak(+)	Strong(+)	Weak(+)	Strong(+)
Her2(-)	3	31 [a]	25	9 [b]
Her2(+)	6	8 [a]	14	0 [b]

Notch attaining was assessed as weak (score, 0 to +2) or strong (+3) expression as described in text. Statistically significant ([a]P=0.0119; [b]P=0.0432).

Table II. Correlation of lymph node metastasis and Notch1 and Notch3 staining.

	Notch1		Notch3	
Metastasis	Weak(+)	Strong(+)	Weak(+)	Strong(+)
LN(-)	2	22 [a]	22	2 [b]
LN(+)	7	17 [a]	17	7 [b]

Lymph node metastasis (LN) was evaluated surgically and histopathologically for presence or absence of tumor cells. Immunostaining was performed for Notch 1 and 3, and the staining was assessed as weak (score, 0 to +2) or strong (+3) expression as described in the text.

detection system (Applied Biosystems) using TaqMan Universal PCR master mix in a 50-ml volume containing 100 nM detection probe and TaqMan gene expression assays of Hes1 (Applied Biosystems). After normalization by glyceraldehyde-3-phosphate dehydrogenase (GAPDH) expression levels, relative expression values of each experiment were calculated by defining the mean value for control as 100%. TaqMan gene expression assays (Applied Biosystems) were used for the detection of Hes1 (Hs01118947_g1) and Gapdh (Hs02758991_g1). Oligo siRNAs of Notch1 (144334; NM_017617), Notch3 (143322; NM_000435), CBF1 (290347; NM_005349), Jagged1 (146915; NM_000214), Jagged2 (11296; NM_002226) were purchased from Ambion-Applied Biosystems, and luciferase from Takara (Kyoto, Japan). To exclude the off-target effect of siRNA, Notch1 (144335; NM_017617), Notch3 (143321; NM_000435), Jagged1 (146914; NM_000214), and Jagged2 (11208; NM_002226) were examined (data not shown).

Protein study and immunohistochemistry. For immunoblot analysis, $5x10^4$ cells in 6-well plates were grown in the medium. Cells were lysed in lysis buffer [20 mM Tris-HCl, 150 mM NaCl, 1 mM EDTA, 1 mM EGTA, 2% NP-40, 2.5 mM sodium pyrophosphate, 1 mM glycerophosphate, 1 mM phenylmethylsulfonyl fluoride, 1 mM sodium orthovanadate, 1 μg/ml leupeptin] for 30 min, centrifuged at 10,000 x g at 4˚C for 20 min. After measuring the concentration of protein using a BioRad kit, 10 μg of protein were separated in 4-20% gradient SDS-PAGE for 2 h at 4˚C, transferred to membrane and probed with primary antibodies, anti-Notch1 intracellular domain and Notch3 (Santa Cruz, Santa Cruz, CA) and Actin (ICN, Irvine CA). The signal was detected with secondary antisera in the ECL system (Amersham, Tokyo, Japan). For immunohistochemistry, after antigen retrieval, endogenous peroxidase was inhibited with 3% hydrogen peroxide, and nonspecific binding sites were blocked with normal goat serum. Slides were incubated overnight with antisera against: Notch1, Notch3, Her2, estrogen receptor (ER) and progesterone receptor (PR) (Santa Cruz Biotechnology) at 1:500, followed by incubation with biotinylated secondary antibody. Slides then were incubated with streptavidin horseradish peroxidase (Dako; 1:1,000). After staining tissues, three independent pathologists observed a hundred low-power fields from each normal epithelium and corresponding cancerous portion, and evaluated the staining intensity of predominant portions as follows: score 0, undetectable or <5% of normal epithelial expression; weak expression (score +1), as 5-50%; within-normal-variations (+2), as 50 and less than the evaluation of +3; strong expression (+3), more than double of normal epithelium.

Statistical analyses. For statistical analysis of significance of differences, the Student's t-test was used. Significant differences when comparing two groups were determined by t-test, $P<0.05$ was considered to be statistically significant. Error bars represent SE.

Results

Overexpression of Notch in Her2-negative primary breast cancer. To characterize the status of Her2 staining in primary breast cancer, the immunohistochemical analysis was performed in 48 surgically obtained tumors. We performed extensive screening assessment of the protein expression of Her2-negative primary breast tumors, compared with receptor-positive tumors, including the status of Notch family, ER, PR, relevant cell membrane and mitochondrial pathways, which allowed the identification of significant association of absent Her2 with the overexpression of Notch proteins (summarized in Tables I and II; the representative staining in Fig. 1). The immunohistochemistry showed that 6 cases of estrogen receptor $(ER)^+$/progesterone receptor $(PR)^+/Her2^+$; 6 cases of $ER^+/PR^-/Her2^-$; none of $ER^-/PR^+/Her2^+$; 4 cases of $ER^-/PR^-/Her2^+$; 22 cases of $ER^+/PR^+/Her2^-$; 4 cases of $ER^+/PR^-/Her2^+$; none of $ER^-/PR^+/Her2^-$; and 6 cases of $ER^-/PR^-/Her2^-$. Her2 was positive in 14 cases (29.2%), whereas Her2 was negative in 34 cases (70.8%).

Notch1 was positive in 40 cases (83.3%), whereas Notch3 was positive in 39 cases (81.3%). The absence of Her2 was associated significantly with the positive staining of Notch1 (p=0.0119) and Notch3 (p=0.0432). The positive staining of Notch3 was relevant with the lymph node metastasis (p=0.1365), showing no significance. Notch1 did not show significant association (p=0.2448). The other assessment, including staining with ER and PR indicates slight significant

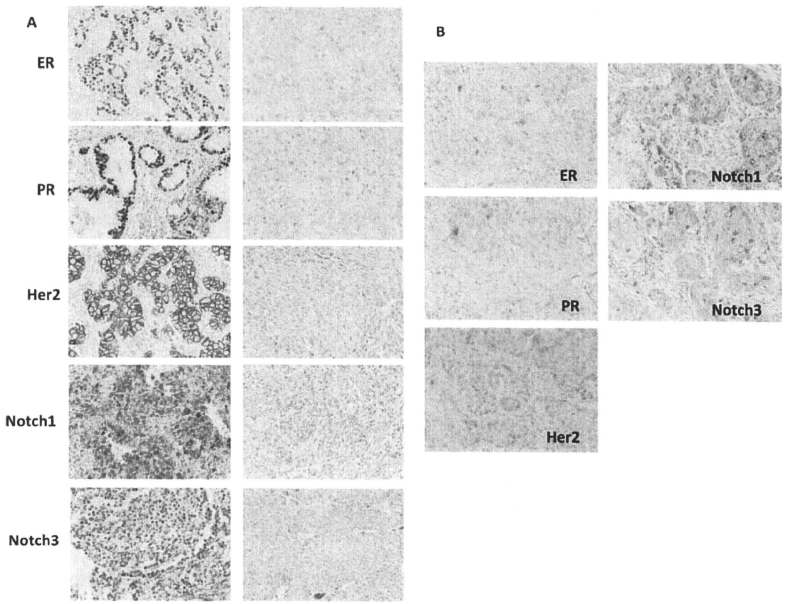

Figure 1. Immunohistochemical detection of Notch pathway and Her2/neu/erbB2 receptor. (A) Representative immunostaining data with specific antibodies (magnification, x200) are shown. Left images indicate strong positive cases for each staining (score, +3, except for Notch3 being +2), whereas those on the right are negative or slightly positive cases (score, 0 to +1). (B) Representative immunostaining data with specific antibodies (magnification, x200) are shown. The tumor region is stained as positive for Notch1 (score, +2) and Notch3 (score, +2), and negative for ER, PR and Her2 (score, 0).

association with the present or absence of Her2 status. The present data indicate the significant association of the absence of Her2 with the overexpression of Notch family, suggesting that, whereas the Her2 could transduce the mitotic signaling in Her2-positive tumors (5), Notch family may play a critical role in breast tumor development, as suggested by the relevant preclinical study of transgenic overexpression of Notch1 and Notch3 that resulted in the development of murine mammary tumors (13), and by studies of Notch in the mammary epithelial cells (10-12).

Activation of Notch pathway. It has been shown that breast cancer tissues are composed of heterogeneous cells with distinct phenotypes, some with stem-cell-like properties, i.e. self-renewing cells with potent tumorigenicity (16,17). Recent studies show that $CD44^+$ breast cancer cells exhibit enhanced invasive properties (18,19). The heterogeneity, similarly to breast cancer (18), was observed also in leukemia (20-22), cancers of the head and neck (23), gastrointestinal system (24), colon (25,26), and brain (27,28). A small population of cancer-initiating cells is potentially very important, because they may play a role in the resistance to genotoxic chemotherapy or radiation therapy and seem be responsible for recurrence after cancer treatments, even when most of the cancer cells appear to be killed and few cancer stem cells remain (29). Although the significance of Notch proteins as stem cell regulatory factors (29) and the radio-resistance property of $CD44^+$ cells (30) have been proposed, exact roles of the Notch family in breast cancer-initiating cells are not yet fully understood.

Here with Her2-negative/dim breast cancer MCF7 and Her2-positive HCC1419 cells (14,15), the expression of Notch1 and Notch3 was studied by immunoblotting. Results indicated that Notch1 and Notch3 proteins were expressed in MCF7 and HCC1419 cells (Fig. 2 and data not shown). It has been reported that breast cancer $CD44^+$ cells exhibit high potential for self-renewal and tumorigenicity, i.e. the properties of breast cancer initiating cells (19,31). $CD44^+$ cells were collected by the MACS and were subjected to immunoblot study. Results of MCF7 indicated that the Notch protein was expressed in $CD44^+$ breast cancer cells and to a slightly lesser extent, in $CD44^-$ fraction; treatment with γ-secretase inhibitor resulted in lower mobility shifting of bands, showing activation of the Notch pathway in the breast cancer cells, and that Notch pathway functions in our system examined (data not shown).

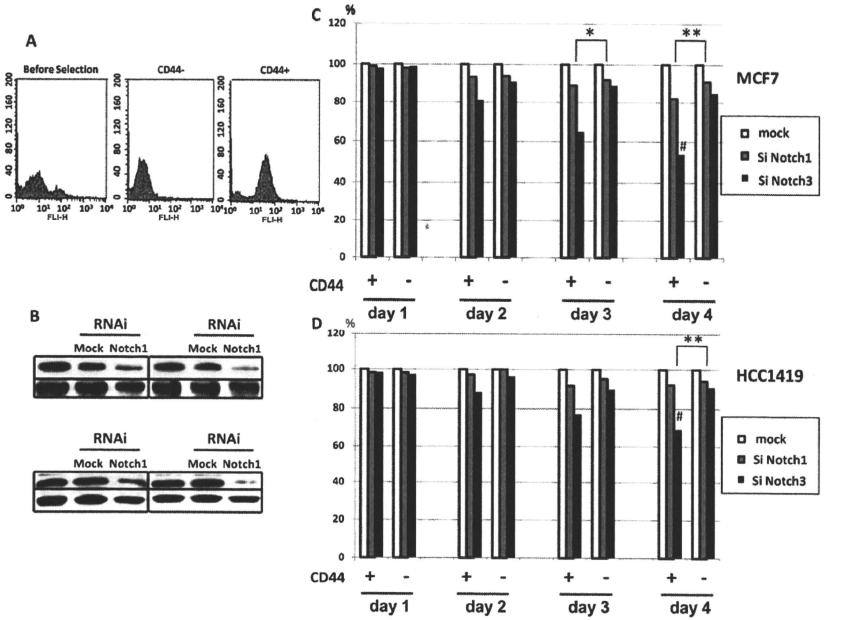

Figure 2. Expression and activation of Notch1 and Notch3 in breast cancer cells. (A) CD44 positive and negative MCF7 cells by FACS analysis. (B) The expression of Notch1 and Notch3. CD44 positive and negative MCF7 were used for immunoblot with anti-Notch1, Notch3 and actin antibodies. The siRNAs knockdown of Notch1 and Notch3 indicate the specificity of the bands. (C and D) MTS proliferation assay of $CD44^+$ and $CD44^-$ breast cancer MCF7 (C) and HCC1419 cells (D), subjected to knockdown of Notch1 and Notch3. The average data were calculated in comparison with the control result with mock treatment and the percent inhibition is shown. The experiment was repeated independently and the representative data are shown. Each character (*, ** and #) indicates statistical significance ($P<0.05$). The characters, + and - indicate the expression status of CD44.

A role of Notch in survival of cancer cells. To study the biological role of the Notch signaling pathway, a knockdown experiment using siRNA was performed. The expression of Notch1 and Notch3 was inhibited by siRNAs but not by treatment with mock siRNAs (Fig. 2; the effect was confirmed by using plural siRNAs), confirming the specificity of Notch1 and Notch3 bands and their significant reduction by siRNA knockdown. An MTS proliferation assay indicated that knockdown of Notch3 resulted in the time-dependent reduction of cell growth of $CD44^+$ MCF7 (inhibition to 52% at day 4, compared with the control) and HCC1419 cells (66%), while the effect of Notch1 knockdown was significantly smaller (82% of MCF7 and 91% of HCC1419). In sharp contrast, the cell growth in $CD44^-$ cells was less reduced by knockdown of Notch1 and Notch3 (84% of MCF7 and 88% of HCC1419 by Notch3 knockdown; 92% of MCF7 and 91% of HCC1419 by Notch1 knockdown at day 4).

Exposure to radiation followed by siRNA inhibition showed that knockdown of Notch3, and to a lesser extent Notch1, elicited a profound reduction of $CD44^+$ cell growth (inhibition to 22% of MCF7 and 28% of HCC1419 by Notch3 knockdown; 71% of MCF7 and 75% of HCC1419 by Notch1 knockdown at day 4, as shown in Fig. 3). The growth inhibitory effect in $CD44^+$ cells by knockdown was appreciably more than the siRNA knockdown in $CD44^-$ (88% of MCF7 and 79% of HCC1419 by Notch3 knockdown; 89% of MCF7 and 81% of HCC1419 by Notch1 knockdown of $CD44^-$ cells).

Inhibition of Notch pathway leading to cancer cell death. To assess the downstream effect of Notch signaling, knockdown experiments of CBF1 and Notch ligands by siRNA were performed by using $CD44^+$ MCF7 and HCC1419 cells (Fig. 4). Results indicated that knockdown of CBF1 resulted in relatively little reduction of cell growth, and that inhibition was enhanced appreciably by the exposure to radiation as a genotoxic insult (inhibition to 78% of MCF7 and 80% of HCC1419 without radiation at day 4; inhibition to 40% of MCF7 and 61% of HCC1419 after radiation). Knockdown of ligand Jagged1 sensitized $CD44^+$ cells to radiation exposure (inhibition to 75% of MCF7 and 82% of HCC1419 without

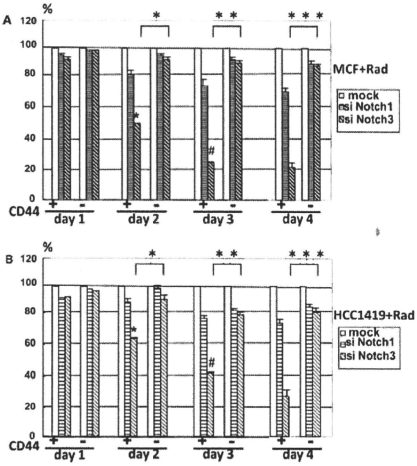

Figure 3. Effect of radiation on MTS proliferation assay. Knockdown of Notch1 and Notch3 in CD44$^+$ and CD44$^-$ breast cancer MCF7 (A) and HCC1419 cells (B) were performed. Each character (*, **, ***, * and #) indicates statistical significance ($P<0.05$). The characters, + and - indicate the expression status of CD44.

radiation; inhibition to 46% of MCF7 and 65% of HCC1419 after radiation). Knockdown of Jagged2 also sensitized CD44$^+$ cells to radiation exposure (inhibition to 76% of MCF7 and 81% of HCC1419 without radiation; inhibition to 50% of MCF7 and 55% of HCC1419 after radiation). To confirm the effect of the Notch signaling pathway, we examined the transcriptional activation of the Hes1 gene by real-time PCR (Fig. 5A). Knockdown of Notch3 and to a lesser extent Notch1 resulted in the reduction of Hes1 transcription [inhibition to 41% by Notch3 knockdown ($P<0.005$); 88% by Notch1 knockdown]. Knockdown of Cbf1, Jagged1 and Jagged2 resulted in the reduction of Hes1 transcription [55% by Cbf1 knockdown ($P<0.005$); 75% by Jagged1 knockdown; 71% by Jagged2 knockdown]. The data showed that the Notch pathway plays a role in regulating the radiosensitivity of CD44$^+$ breast cancer cells.

To study the growth reduction of breast cancer cells to radiation exposure, the evaluation of sub-G1 fraction by a flow cytometry was performed (Fig. 5B). Propidium iodide staining indicated that Notch3, Cbf1 and to a lesser extent Notch1 induced an increase in sub-G1 fraction in CD44$^+$ breast cancer cells after radiation exposure, whereas sub-G1 was less induced in the absence of radiation (40, 22 and 15% after radiation; 21, 8 and 3% of subG1 by Notch3, Notch1 and mock, without radiation, respectively). These data showed that the growth inhibition induced by knockdown of the Notch pathway after radiation exposure resulted in sensitization of cells to the induction of apoptosis.

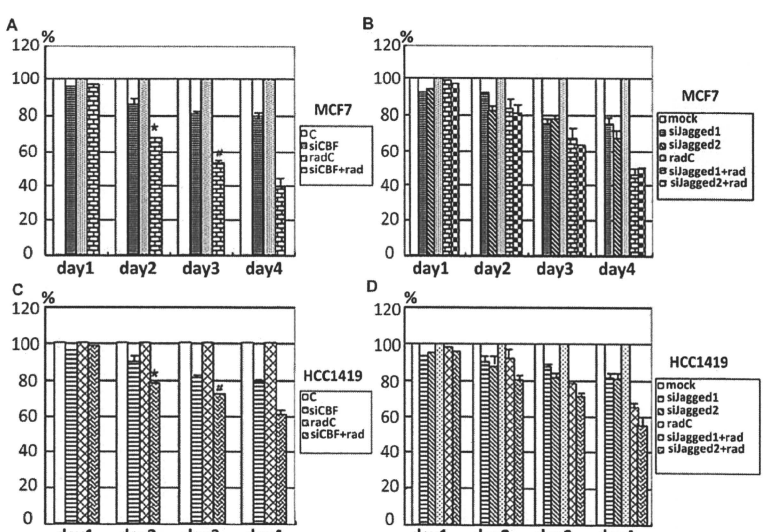

Figure 4. Knockdown of CBF1 and ligands Jagged1 and Jagged2 in breast cancer cells. MCF7 (A and C) and HCC1419 cells (B and D) were used. MTS proliferation assay of CD44$^+$ breast cancer cells with knockdown of CBF1 and ligands Jagged1 and Jagged2, with and without radiation exposure. Each character (* and #) indicates statistical significance ($P<0.05$).

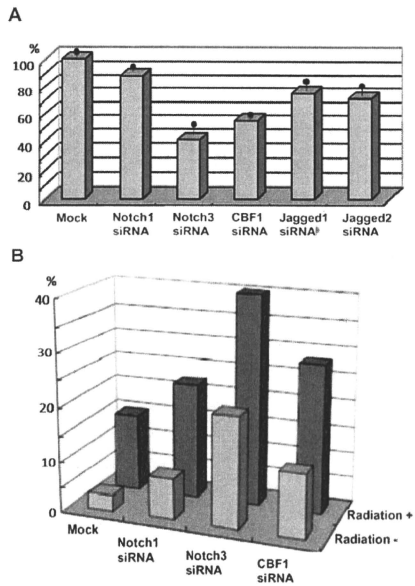

Figure 5. Study of the Notch pathway. (A) Real-time PCR data of the transcriptional target of the Notch pathway, Hes1. Knockdown of Notch1, Notch3, CBF1, Jagged1, and Jagged2 were performed and subjected to real-time PCR. Data are shown as % amounts of amplification compared with mock experiment. Bar with dot indicates SE. (B) Apoptosis of breast cancer initiating cells. $CD44^+$ MCF7 cells were treated with siRNAs of Notch1, Notch3 and Cbf1, with or without radiation exposure. The sub-G1 fraction (%) by FACS analysis is shown.

Discussion

Our data suggest that Notch would be a candidate therapeutic target for cancer-initiating cells, i.e. the inhibition and sensitization of $CD44^+$ breast cancer cells to radiation. We found that Notch3 and Notch1 knockdown reduced the transactivation of the Hes1 gene, although a protein homology search indicated that Notch3 lacks the putative transactivation domain of Notch1, suggesting that the domain may be dispensable. This is compatible with previous studies that Notch transactivations are complex mechanisms, and the downstream regulation of Notch3 remains to be elucidated fully (10,32). A previous study showed that mouse Notch3 knockout mice are viable and fertile, although Notch3 is required for arterial identity and maturation of vascular smooth muscle cells and the mice exhibit cardiovascular defects (33). In contrast, Notch1 is required for the coordinate segmentation of somites and Notch1-deficient mice showed early embryonic lethality (34,35). It is thus suggested that Notch1 plays an indispensable role in development and targeting Notch1 in cancer therapy might lead to severe toxic side effects. The inhibition of Cbf1 and ligands might elicit unexpected side effects, considering that those factors are cross-talking among the Notch family. Notch3 is proposed as a candidate therapeutic target of cancer-initiating cells.

The resistance of cancer initiating cells to chemotherapy generally has been shown to be associated with various types of ATP-binding cassette (ABC) transporters, which contribute to drug resistance in many cancers by pumping chemotherapy reagents out of cells (24,36). Also, the checkpoint activation Chk1/Chk2 pathway is reported to be involved in the radioresistance of brain tumor-initiating cells (37). The checkpoint activity in damaged cells after genotoxin stress may be involved in the aberrant repairs, which can contribute to the step-wise accumulations of genomic instability in cancerous cells and presumably cancer stem cells, as suggested by genomic studies of embryonic tumor cells (38) and glioma stem cells (27), and functional assessment of tumor suppressor Fhit (39-41). Based on the present study, one could speculate that Notch plays a role in maintaining the growth of breast cancer-initiating cells, which could offset radiation-induced cancer cell death, and Notch could be a candidate target for therapy aimed at the radiosensitization of Her2-negative $CD44^+$ breast cancer stem cells. In addition, our data indicate that MCF7 cells show a profound reduction of cell growth after the knockdown of Notch3 and Cbf1, whereas the ErbB2 protein was substantially expressed in HCC1419 but undetectable in MCF7 cells, suggesting that multiple marker status, including ErbB2, estrogen-receptor, and CD24, might define Notch-dependency of cancer-initiating cells responding to genotoxic therapy. The present study furnishes the rationale for us to study further efficient targeting cancer-initiating cells, which could overcome the cytoreduction therapy-resistance.

Previous study to determine population-based distributions and clinical associations in 496 incident cases of breast cancer subtypes indicated that basal-like breast tumors with Her2/ER/PR-triple negative status occurred at a higher prevalence among premenopausal African American patients compared with postmenopausal African American and non-African American patients (42). In this context, recent study indicates that mesenchyme Forkhead 1 (Foxc2) transcription factor plays a central role in promoting invasion and metastasis and that it may prove to be a highly specific molecular marker for human basal-like breast cancers, via the mechanism of epithelial-mesenchymal transitions (EMTs) (43), of which a transdifferentiation program often activate carcinoma cells to acquire the ability to execute the multiple steps of the invasion-metastasis cascade, triggered by a number of signals, including transforming growth factor-1 and several EMT-inducing transcription factors, such as Snail, Twist, Goosecoid, and Jagged-Notch pathways (44,45). Our findings indicate the candidacy of the Notch pathway as the target for therapeutic control of growth and differentiation of Her2-negative breast cancer-initiating cells and suggest the rationale for further investigation.

Recently it was reported that, in Brca1/Brca2-deficient and Her2/ER/PR-triple-negative breast cancer cells, the DNA damage signaling kinase Ataxia-telangiectasia-mutated is aberrantly reduced or lost (46), indicating a model of the accumulation of genomic instability under conditions of enhanced DNA damage in precancerous, cancer-initiating

lesions resulting in more robust activation and hence increased selection for inactivation or loss of repair and cell death with tumors of haploinsufficient Brca1/2 mutation carriers, with implications for curability of diverse subsets of human breast cancer.

The present study demonstrates the significance of the Notch pathway, which plays a role in signal transduction of pro-survival of $CD44^+$ breast cancer-initiating cells carrying deleterious damage, indicating that survival signal such as maintenance of the stemness is involved in development of cancer-initiating cells with increasing genomic instability. We have shown that Notch plays a role in the regulation of Her2-negative breast cancer initiating cells after radiation exposure, suggesting that targeted suppression of the Notch signaling pathway in breast cancer-initiating cells may be useful for sensitizing Her2-negative tumor to a therapeutic approach. The high-level co-expression of Jagged1 and Notch1 in human breast cancer has also been shown (47). Although others have reported the associations between Notch-2, Akt-1 and Her2/neu expression (48) and the high-level expression of Jag1 in human breast cancer (49,50), the present study supports the critical and novel concept that Notch pathway plays a role in Her2-negative breast cancer initiating cells.

References

1. Montgomery DA, Krupa K and Cooke TG: Follow-up in breast cancer: does routine clinical examination improve outcome? A systematic review of the literature. Br J Cancer: 97: 1632-1641, 2007.
2. Coleman MP, Rachet B, Woods LM, *et al*: Trends and socio-economic inequalities in cancer survival in England and Wales up to 2001. Br J Cancer 90: 1367-1373, 2004.
3. Karamouzis MV, Konstantinopoulos PA and Papavassiliou AG: Trastuzumab - mechanism of action and use. N Engl J Med 357: 1664-1666, 2007.
4. Bange J, Zwick E and Ullrich A: Molecular targets for breast cancer therapy and prevention. Nature Med 7: 548-552, 2001.
5. Menard S, Pupa SM, Campiglio M and Tagliabue E: Biologic and therapeutic role of HER2 in cancer. Oncogene 22: 6570-6578, 2003.
6. Kute T, Lack CM, Willingham M, *et al*: Development of Herceptin resistance in breast cancer cells. Cytometry A 57: 86-93, 2004.
7. Tan AR and Swain SM: Ongoing adjuvant trials with trastuzumab in breast cancer. Semin Oncol 30 (Suppl 16): 54-64, 2002.
8. Bray S: Notch signalling: a simple pathway becomes complex. Nat Rev Mol Cell Biol 7: 678-689, 2006.
9. Artavanis-Tsakonas S, Rand MD and Lake RJ: Notch signaling: Cell fate control and signal integration in development. Science 284: 770-776, 1999.
10. Miele L, Golde T and Osborne B: Notch signaling in cancer. Curr Mol Med 6: 905-918, 2006.
11. Shi W and Harris AL: Notch signaling in breast cancer and tumor angiogenesis: cross-talk and therapeutic potentials. J Mammary Gland Biol Neoplasia 11: 41-52, 2006.
12. Efstratiadis A, Szabolcs M and Klinakis A: Notch, Myc and breast cancer. Cell Cycle 6: 418-429, 2007.
13. Hu C, Dievart A, Lupien M, Calvo E, Tremblay G and Jolicoeur P: Overexpression of activated murine Notch1 and Notch3 in transgenic mice blocks mammary gland development and induces mammary tumors. Am J Pathol 168: 973-990, 2006.
14. Corsini C, Mancuso P, Paul S, Burlini A, Martinelli G, Pruneri G and Bertolini F: Stroma cells: a novel target of herceptin activity. Clin Cancer Res 9: 1820-1825, 2003.
15. Chrestensen CA, Shuman JK, Eschenroeder A, Worthington M and Gram H: MNK1 and MNK2 regulation in HER2-overexpressing breast cancer lines. J Biol Chem 282: 4243-4252, 2007.
16. Dontu G, Liu S and Wicha MS: Stem cells in mammary development and carcinogenesis: implications for prevention and treatment. Stem Cell Rev 1: 207-213, 2005.
17. Ponti D, Zaffaroni N, Capelli C and Daidone MG: Breast cancer stem cells: an overview. Eur J Cancer 42: 1219-1224, 2006.
18. Al-Hajj M, Wicha MS, Benito-Hernandez A, Morrison SJ and Clarke MF: Prospective identification of tumorigenic breast cancer cells. Proc Natl Acad Sci USA 100: 3983-3988, 2003.
19. Sheridan C, Kishimoto H, Fuchs RK, *et al*: $CD44^+/CD24^-$ breast cancer cells exhibit enhanced invasive properties: an early step necessary for metastasis. Breast Cancer Res 8: R59, 2006.
20. Lapidot T, Sirard C, Vormoor J, *et al*: A cell initiating human acute myeloid leukemia after transplantation into SCID mice. Nature 367: 645-648, 1994.
21. Bonnet D and Dick JE: Human acute leukemia is organized as a hierarchy that originates from a primitive hematopoietic cell. Nat Med 3: 730-737, 1997.
22. Wulf GG, Wang RY, Kuehnle I, *et al*: A leukemic stem cell with intrinsic drug efflux capacity in acute myeloid leukemia. Blood 98: 1166-1173, 2001.
23. Prince ME, Sivanandan R, Kaczorowski A, *et al*: Identification of a subpopulation of cells with cancer stem cell properties in head and neck squamous cell carcinoma. Proc Natl Acad Sci USA 104: 973-978, 2007.
24. Haraguchi N, Utsunomiya T, Inoue H, Tanaka F, Mimori K, Barnard GF and Mori M: Characterization of a side population of cancer cells from human gastrointestinal system. Stem Cell 24: 506-513, 2006.
25. O'Brien CA, Pollett A, Gallinger S and Dick JE: A human colon cancer cell capable of initiating tumour growth in immuno-deficient mice. Nature 445: 106-110, 2007.
26. Ricci-Vitiani L, Lombardi DG, Pilozzi E, Biffoni M, Todaro M, Peschle C and De Maria R: Identification and expansion of human colon-cancer-initiating cells. Nature 445: 111-115, 2007.
27. Bao S, Wu Q, McLendon RE, *et al*: Glioma stem cells promote radioresistance by preferential activation of the DNA damage response. Nature 444: 756-760, 2006.
28. Piccirillo SG, Reynolds BA, Zanetti N, *et al*: Bone morphogenetic proteins inhibit the tumorigenic potential of human brain tumour-initiating cells. Nature 444: 761-765, 2006.
29. Tan BT, Park CY, Ailles LE and Weissman IL: The cancer stem cell hypothesis: a work in progress. Lab Invest 86: 1203-1207, 2006.
30. Phillips TM, McBride WH and Pajonk F: The response of $CD24^{(-/low)}/CD44^+$ breast cancer-initiating cells to radiation. J Natl Cancer Inst 98: 1777-1785, 2006.
31. Gotte M and Yip GW: Heparanase, hyaluronan, and CD44 in cancers: a breast carcinoma perspective. Cancer Res 66: 10233-10237, 2006.
32. Anderson LM and Gibbons GH: Notch: a mastermind of vascular morphogenesis. J Clin Invest 117: 299-302, 2007.
33. Domenga V, Fardoux P, Lacombe P, *et al*: Notch3 is required for arterial identity and maturation of vascular smooth muscle cells. Genes Dev 18: 2730-2735, 2004.
34. Conlon RA, Reaume AG and Rossant J: Notch1 is required for the coordinate segmentation of somites. Development 121: 1533-1545, 1995.
35. Huppert SS, Ilagan MX, De Strooper B and Kopan R: Analysis of Notch function in presomitic mesoderm suggests a gamma-secretase-independent role for presenilins in somite differentiation. Dev Cell 8: 677-688, 2005.
36. Lou H and Dean M: Targeted therapy for cancer stem cells: the patched pathway and ABC transporters. Oncogene 26: 1357-1360, 2007.
37. Hambardzumyan D, Squatrito M and Holland EC: Radiation resistance and stem-like cells in brain tumors. Cancer Cell 10: 454-456, 2006.
38. Lin Q, Donahue SL and Ruley HE: Genome maintenance and mutagenesis in embryonic stem cells. Cell Cycle 5: 2710-2714, 2006.
39. Ottey M, Han SY, Druck T, *et al*: Fhit-deficient normal and cancer cells are mitomycin C and UVC resistant. Br J Cancer 91: 1669-1677, 2004.
40. Hu B, Han SY, Wang X, *et al*: Involvement of the Fhit gene in the ionizing radiation-activated ATR/CHK1 pathway. J Cell Physiol 202: 518-523, 2005.
41. Hu B, Wang H, Wang X, *et al*: Fhit and CHK1 have opposing effects on homologous recombination repair. Cancer Res 65: 8613-8616, 2005.

42. Carey LA, Perou CM, Livasy CA, *et al*: Race, breast cancer subtypes, and survival in the Carolina Breast Cancer Study. JAMA 295: 2492-2502, 2006.
43. Bailey JM, Singh PK and Hollingsworth MA: Cancer metastasis facilitated by developmental pathways: Sonic hedgehog, Notch, and bone morphogenic proteins. J Cell Biochem 102: 829-839, 2007.
44. Fidler I: The pathogenesis of cancer metastasis: the 'seed and soil' hypothesis revisited. Nat Rev Cancer 3: 453-458, 2003.
45. Mani SA, Yang J, Brooks M, *et al*: Mesenchyme Forkhead 1 (FOXC2) plays a key role in metastasis and is associated with aggressive basal-like breast cancers. Proc Natl Acad Sci USA 104: 10069-10074, 2007.
46. Tommiska J, Bartkova J, Heinonen M, *et al*: The DNA damage signalling kinase ATM is aberrantly reduced or lost in BRCA1/BRCA2-deficient and ER/PR/ERBB2-triple-negative breast cancer. Oncogene 27: 2501-2506, 2008.
47. Reedijk M, Odorcic S, Chang L, *et al*: High-level coexpression of JAG1 and NOTCH1 is observed in human breast cancer and is associated with poor overall survival. Cancer Res 65: 8530-8537, 2005.
48. Florena AM, Tripodo C, Guarnotta C, *et al*: Associations between Notch-2, Akt-1 and HER2/neu expression in invasive human breast cancer: a tissue microarray immunophenotypic analysis on 98 patients. Pathobiology 74: 317-322, 2007.
49. Dickson BC, Mulligan AM, Zhang H, Lockwood G, O'Malley FP, Egan SE and Reedijk M: High-level JAG1 mRNA and protein predict poor outcome in breast cancer. Mod Pathol 20: 685-693, 2007.
50. Reedijk M, Pinnaduwage D, Dickson BC, *et al*: JAG1 expression is associated with a basal phenotype and recurrence in lymph node-negative breast cancer. Breast Cancer Res Treat 111: 439-448, 2008.